Available online at www.sciencedirect.com
SCIENCE DIRECT
Journal of Sound and Vibration 295 (2006) 141–164
JOURNAL OF SOUND AND VIBRATION
www.elsevier.com/locate/jsvi

Analysis of the relation between injection parameter variation and block vibration of an internal combustion diesel engine

A.P. Carlucci*, F.F. Chiara, D. Laforgia

Research Center for Energy and Environment (CREA), University of Lecce, via per Arnesano 73100 Lecce, Italy

Received 13 December 2004; received in revised form 5 December 2005; accepted 20 December 2005
Available online 17 April 2006

Abstract

The development of combustion in diesel engines is strictly dependent on injection parameters, like injection number and timings, fuel quantity and mean injection pressure. Moreover, it is well known that the variation of the injection parameters has an effect on the engine block vibration. Hence, the present work aims at investigating the possibility of using engine block vibration as a mean to diagnose, outwardly, the combustion modifications induced by these parameters. So, the possibility of following the combustion modifications by means of two accelerometers positioned at two different zones of the engine block has been analysed, defining a characteristic "signature" for each parameter. Classical Fourier analysis and time–frequency analysis were used to define the degree of correlation between in-cylinder pressure and vibration signals. It has been proved that injection pressure and injected quantities, over an energy release threshold, really affect the vibration signals in a peculiar way; injection timing affects the engine block vibration in a less evident way, but a characteristic signature was also defined for this factor.
© 2006 Elsevier Ltd. All rights reserved.

1. Introduction

The need to minimize long and expensive machine failures on the application in which the same machines play a crucial role has directed research towards the study of new monitoring and diagnostic techniques based on non-intrusive methods.

If, generally speaking, these techniques are now well-established tools for rotating machines, like compressors, turbines, pumps and power generators; this cannot be said for the internal combustion engines.

Besides, as for internal combustion engines, the new regulations demanding higher efficiency in terms of emission and fuel consumption reduction, guide the technological development towards more advanced injection systems. This is because the fuel injection mode, that determines fuel droplet dimensions and related spatial distribution inside the combustion chamber, strongly affects the ignition, combustion and pollutant formation processes. The high technological content of high-performance injection systems implies a higher degree of perishability, especially in adverse surroundings, as the combustion chamber of an internal combustion engine.

*Corresponding author. Tel.: +39 0832 297370; fax: +39 0832 297279.
E-mail address: paolo.carlucci@unile.it (A.P. Carlucci).

0022-460X/$ - see front matter © 2006 Elsevier Ltd. All rights reserved.
doi:10.1016/j.jsv.2005.12.054

Among the different diagnostic techniques tested to analyse misfiring, Azzoni et al. [1] proposed an indicator based on the crankshaft velocity fluctuations. This indicator is a function of the amplitudes of the zeroth, first, and second orders of engine cycle components, resulting from the angular velocity signal sampled on a cycle-by-cycle basis and computed through a discrete Fourier transform. The authors proved that this indicator is able to distinguish with sufficient precision the occurrence of misfire, operating the engine in both stationary and acceleration and deceleration conditions.

Ball et al. [2,3] tested a diagnostic system based on the measurement of environmental noise. The sensitivity of the indicator, derived from the continuous wavelet transform, was shown to some simulated malfunctioning, like a reduction of either the volumetric compression ratio or the opening pressure of the injector. However, it was underlined that further improvements of the diagnosis method were required in order to distinguish among the different kinds of malfunctioning. Among the diagnostic techniques applied to internal combustion engines, those based on the analysis of accelerometer data have earned a greater success. Chun and Kim [4] showed the possibility of obtaining a measure of a spark ignition engine knock analysing the oscillations measured at the upper part of the cylinder block center. Zurita et al. [5], on the contrary, rebuilt the in-cylinder pressure history through the signal provided by an accelerometer placed externally. Then, the in-cylinder pressure trend was used as a diagnostic tool. Othman [6] used an accelerometer horizontally mounted on the side wall of a spark ignition engine to monitor the combustion anomalies, like misfiring, and to adjust automatically the air–fuel ratio and the ignition time of the spark plug. Antoni et al. [7] suggested the analysis of an internal combustion engine vibrations using cyclostationarity to overcome the vibration non-stationarity. This approach, combined with the synchronous sampling and not time sampling, makes possible the definition of some malfunctioning indicators, like knock or misfiring. This approach, however, revealing the presence of a malfunction, often did not supply useful information about its nature. Schmillen and Wolschendorff [8] pointed out that the pressure oscillation amplitude inside the combustion chamber (and the combustion noise of the diesel engine, as a consequence), was strongly dependent on the duration of the ignition delay. In fact, the longer this duration, the more are the sites in the combustion chamber where simultaneous autoignition takes place. This energy release, not uniform in space and time, causes in-cylinder pressure oscillations, not uniform in space and time either. Starting from these remarks, Blunsdon and Dent [9] figured out numerically the temporal trends of the in-cylinder pressure at different locations of the combustion chamber varying the injection profile, the number of subsequent injections, the timing of the different injections, the swirl ratio, the injector position, and the thermal boundary conditions. The results showed that these variables strongly affect the bulk motion settling inside the combustion chamber.

The aim of the present work is to analyse the possibility of diagnosing the cause of a malfunction, in particular of the injection system, through the analysis of accelerometer data. In fact, the strong correlation between injection parameters, in-cylinder pressure field and vibrations induced on the external surface of the engine, suggests the possibility of obtaining useful information for the diagnosis of the engine malfunction analysing the variation of the accelerometer measured profiles.

2. The engine and the experimental set-up

The tests were carried out on a four cylinder, D.I, FIAT 1929 cm^3 TDID 154 D 1.000 Diesel engine, turbocharged with a GARRETT TD 2502 and equipped with a common rail (Bosch 1350 bar) injection system. This system was operated by a control unit to modify the injection parameters, like injection strategy (single or multiple injection), injection timings, durations and pressures. The engine and injection system main characteristics are reported in Table 1. The engine was mounted to two steel crossbars connected to a steel platform by means of four steel supports.

The engine tests have been carried out at constant load and speed. These parameters were controlled by an eddy-current dynamometer ZÖLLNER-KIEL type ALPHA 160 AF, connected to the engine through an elastic coupling. The acceleration of the cylinder block was measured by two piezoelectric accelerometers KISTLER K SHEAR 8704B100, powered by a single-channel coupler KISTLER type 5118B2. The first accelerometer (a_1) was placed horizontally on the side wall of the block, close to cylinder No. 4 whose pressure was acquired; the second one (a_2) was placed vertically on the camshaft cover close to cylinder No. 4. Both the

Table 1
Test engine and fuel injection equipment specification

Engine specifications	
Total number of cylinders	4
Total displacement	1930 cm^3
Maximum power	69 kW
Maximum torque	200 Nm
Minimum speed	950 rev/min
Maximum speed	4950 rev/min
Bore	82.6 mm
Stroke	90 mm
Compression ratio	19.8 ± 0.8
Inlet valve opening	0° BTDC
Inlet valve closure	32° ABDC
Exhaust valve opening	32° BBDC
Exhaust valve closure	0° ATDC
Fuel injection equipement specifications	
Injector type	Electro-hydraulically controlled
Injection pressure	Variable up to 135 MPa
Nozzle type	VCO
Number of nozzle holes	5
Hole diameter	0.18 mm
Hole L/D ratio	6
Included spray angle	145°

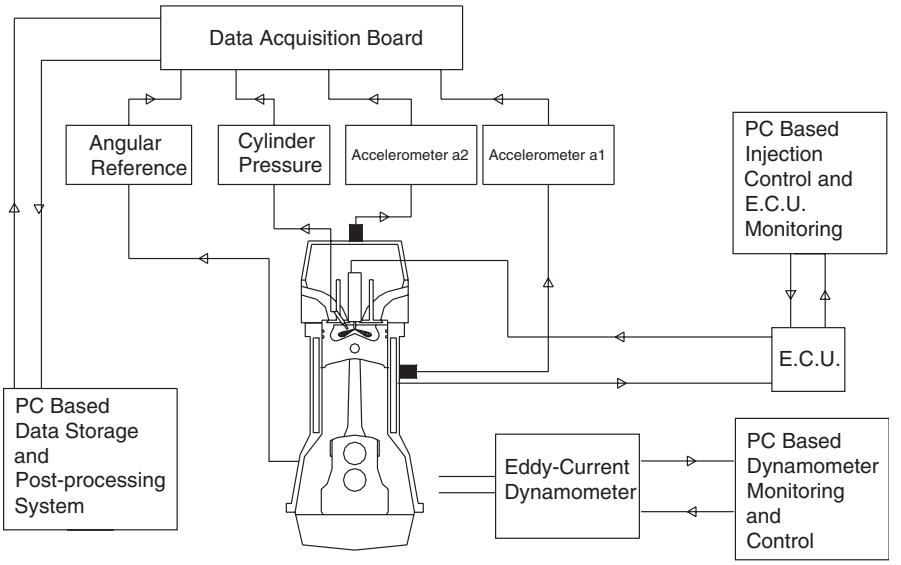

Fig. 1. Experimental set-up.

accelerometers were firmly fixed by means of threaded pins. Fig. 1 shows the experimental layout and the accelerometer positioning.

The in-cylinder pressure was acquired using a piezoelectric transducer, KISTLER type 6053, connected by a charge amplifier to the acquisition board.

The voltage signals of the accelerometers, the pressure transducer, and the one related to the energizing current of the electro-injectors were sampled with an acquisition board NI type 4472, with a peak acquisition frequency of 100 kHz per channel and an anti-aliasing filter. The sampling frequency used for all the

Table 2
Accelerometer and pressure transducer technical data

Accelerometer specifications		
Sensor type	—	Piezoelectric
Measuring range	(g)	± 100
Sensitivity	(mV/g)	50
Natural frequency	(kHz)	50
Transverse sensitivity	(%)	1.5
Pressure transducer specifications		
Sensor type	—	Piezoelectric
Measuring range	(bar)	0–250
Sensitivity	(pC/bar)	−19
Natural frequency	(kHz)	130
Linearity	(%FSO)	$< \pm 0.5$

aforementioned signals was 50 kHz. The accelerometer and pressure transducer main features are summarized in Table 2.

3. The in-cylinder pressure as the basic force

Diesel engine combustion can be schematically divided in three stages [10]: the first one, called ignition delay, in which the fuel injected in the combustion chamber accumulates without burning; the second one, in which a sudden development of the combustion of the premixed charge takes place; and the third one, in which the combustion of the remaining portion of the fuel injected develops in heterogeneous phase, called diffusive combustion. The harshness, which is the distinctive aspect of diesel combustion, is caused by the sudden development of the combustion of the premixed charge formed during the ignition delay.

In the past, great attention was addressed to study a method to characterize the time diagram of the in-cylinder pressure to predict its effects on block vibration and engine noise. Some of these methods consider the peak value or alternatively the first or second derivative of the in-cylinder pressure. As a matter of fact, the in-cylinder pressure peak value clearly affects the low-frequency components, while the highest frequency harmonics are directly related to the shape of the pressure history. In particular, the sudden detachment from the motored pressure curve, due to the early stage of the combustion process, produces a steep fronted wave that, spreading inside the combustion chamber, causes charge and pressure oscillations, source of high-frequency peaks on the in-cylinder pressure spectrum.

The frequency content of a generic signal $x(t)$ can be pointed out using the related Auto-Power Spectral Density Function (PSD) S_{xx}, consisting of the Fourier transform of the autocorrelation function, computed through [11]

$$S_{xx}(f) = \int_{-\infty}^{+\infty} \left[E\{x(t)x(t+\tau)\}\right] e^{-j2\pi f\tau}\, d\tau, \tag{1}$$

where the expression in square brackets is defined as the autocorrelation function and indicated $R_{xx}(\tau)$:

$$R_{xx}(\tau) = E\{x(t)x(t+\tau)\}. \tag{2}$$

The autocorrelation function $R_{xx}(\tau)$ of a given signal $x(t)$ can be read as a measure of the degree of certainty by means of which future values of the signal can be calculated by the knowledge of the previous ones. If the probability density function $p(x)$ of the data $x(t)$ is known, the degree of probability with which future values are included in a given range of possible values can be estimated. The greater the random nature of the signal, the faster the decaying time of the autocorrelation function with the increase of τ, whose meaning is the low predictability of future values of the signal.

Given the symmetry properties of the autocorrelation function ($R_{xx}(-\tau) = R_{xx}(\tau)$), it is more appropriate to consider the one-sided PSD defined by

$$G_{xx}(f) = \begin{cases} 2S_{xx}(f) & f > 0, \\ S_{xx}(f) & f = 0, \\ 0 & f < 0. \end{cases} \tag{3}$$

The one-sided PSD, often used in real applications, can be read as a measure of the rate of variation of the root mean square (RMS) of data varying the frequency. In fact, the key relation to correctly explain the meaning of the PSD is given just by the relation between the last one and the RMS of the signal:

$$\mathrm{RMS}_x(f_1, f_2) = \int_{f_1}^{f_2} G_{xx}(f)\,\mathrm{d}f, \tag{4}$$

where f_1 and f_2 define a frequency interval.

The previous relation refers to time records of infinite length, T being of infinite length. As a matter of fact, real signal acquisitions have to be of finite length; furthermore, it has to be pointed out that data-acquisition techniques are based on digital methods, and for this reason, from now on, it will be assumed that all the quantities referred, were computed through evaluation methods based on digital finite records.

In Fig. 2 the typical PSD of the in-cylinder pressure for an engine speed of 1400 rev/min is shown. It can be observed that, beyond the initial part of the diagram, showing a nearly straight trend, due to the high density of the components related to the frequency combustion, the high-frequency peaks, due to the resonant oscillations of the charge are clearly detectable.

In order to relate the quantities derived from accelerometer signals with the combustion development, the rate of heat release (ROHR), directly related to the in-cylinder pressure curve, was computed through a classical thermodynamic single-zone model. This model (Eq. (5)) is obtained by the application of the first law of thermodynamics [10].

$$\mathrm{ROHR}(\theta) = \frac{\gamma}{\gamma - 1} p \frac{\mathrm{d}V(\theta)}{\mathrm{d}\theta} + \frac{1}{k - 1} V \frac{\mathrm{d}p(\theta)}{\mathrm{d}\theta} \tag{5}$$

In Eq. (5), $V(\theta)$ is the chamber volume at the crank angle θ, $p(\theta)$ is the in-cylinder pressure value measured at the same crank angle and γ is specific heat ratio.

As already said, the present paper deals with the possibility to detect, through the engine block vibration monitoring, a typical "signature" induced by a particular injection parameter variation. Therefore, a complete four-parameter factorial experimental plan, reported on Table 3, was carried out. The varied injection parameters were: pilot injection timing (AiP), pilot injection energizing time (ETP), main injection timing (A_i) and mean injection pressure (p_{inj}). Each of these parameters, whose values are summarized in Table 4, is expected to affect in a peculiar way the combustion process, somehow modifying the rate of variation of the

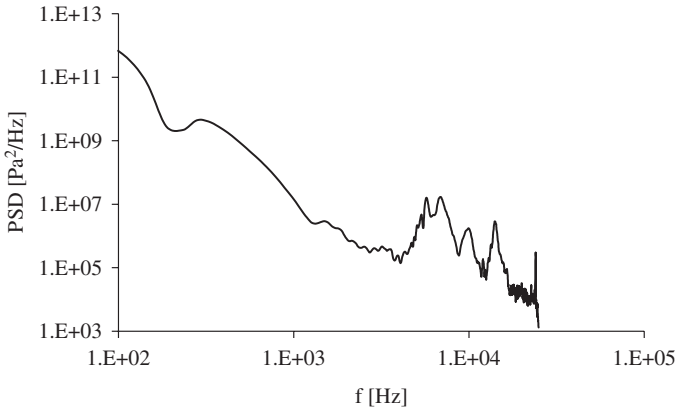

Fig. 2. PSD modulus of the in-cylinder pressure signal.

Table 3
Four factors complete factorial plan

Test	AiP	ETP	A_i	p_{inj}
1	0	0	0	0
2	0	0	0	1
3	0	0	1	0
4	0	0	1	1
5	0	1	0	0
6	0	1	0	1
7	0	1	1	0
8	0	1	1	1
9	1	0	0	0
10	1	0	0	1
11	1	0	1	0
12	1	0	1	1
13	1	1	0	0
14	1	1	0	1
15	1	1	1	0
16	1	1	1	1

Table 4
Injection control factors

Parameter	Level 0	Level 1
Pilot injection timing (AiP)	19° BTDC	23° BTDC
Pilot injection ET (ETP)	150 μs	200 μs
Main injection timing (A_i)	3° BTDC	0° BTDC
Injection pressure (p_{inj})	60 MPa	100 MPa

in-cylinder pressure and the related frequency distribution. From now on, all the tests will be identified using the notation [AiP]/[ETP]/[A_i]/[p_{inj}], in which the quantities in square brackets have been previously defined.

4. Preliminary treatment of the signals

Both the accelerometer and the in-cylinder pressure signals were processed, in order to exclusively show up an interval of 180° around the top dead center (TDC) corresponding to the end of the compression stroke of the cylinder No. 4. This angular windowing is needed to isolate the vibration signal components only, due to the combustion on the cylinder in which the in-cylinder pressure was detected, leaving out the contribution of the combustion in the adjacent cylinders.

In particular, Fig. 3 presents all sampled signals after the time windowing operation, while Fig. 4 underlines that in the aforementioned angle interval, the combustion inside the cylinder No. 4 is the only one that takes place. Therefore, it is possible to recognize the purely mechanical events distinguishing them from those caused by the combustion process. Although the signals were acquired with a temporal basis, the good operating stability of the engine made it possible to convert them to the angular domain. In this way, it was possible to move all the analysis from time to angle domain, a more appropriate approach for the classification of the events related to the engine working conditions, as was also underlined in Ref. [7].

5. Signal analysis

It is quite complicated to perform classical Fourier analysis on internal combustion engine vibration signals, because the combustion frequency content, recognizable but concentrated in a short-time interval, is

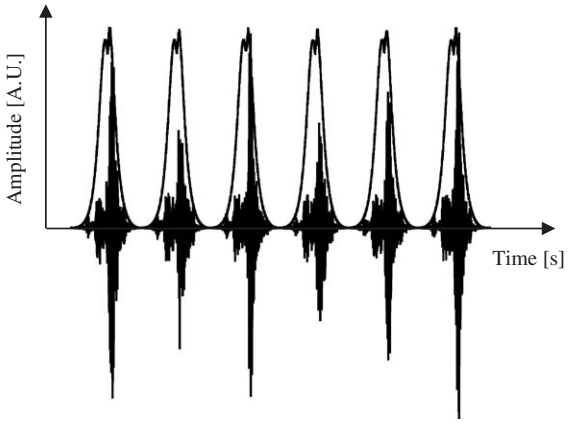

Fig. 3. Generic sampling of the in-cylinder pressure, accelerometer a_1 and a_2, after the windowing.

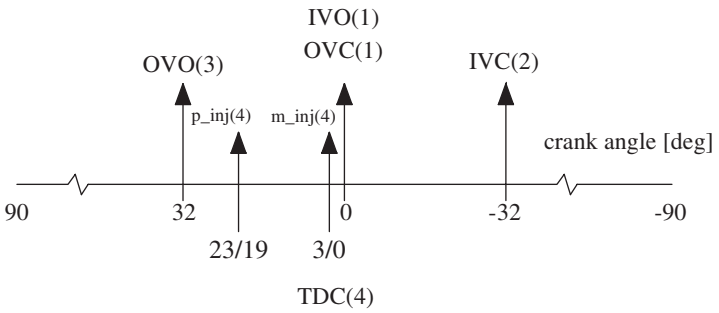

Fig. 4. Theoretical occurrences of inlet valve opening (IVO) and closure (IVC), output valve opening (OVO) and closure (OVC), pilot injection (p_{inj}) and main injection (m_{inj}) start for the cylinder in round brackets.

distributed and then smoothed on the cycle period. Therefore, more appropriate analysis tools, like time–frequency analysis, are needed, together with those aforementioned, to define in the time domain the signal frequency content. Keeping in mind the object of the present work, the use of engine block vibrations as a diagnostic tool, the time–frequency analysis will not be employed as the final term of the line of reasoning but as a tool to give physical sense to quantities, coupling ease of calculation with quick comprehension.

The time–frequency analysis was performed on averaged data, meaning that, the signals provided by the two accelerometers were averaged using, as suggested in Ref. [7], the following relation:

$$s(m) = \frac{1}{I}\sum_{i=0}^{I-1} s(m + iN), \tag{6}$$

where I is the number of signal periods, N is the number of the samples for one signal period and m refers to the sample at the generic angle position. Starting from this signal, time–frequency analysis was carried out employing the short-time Fourier transform (STFT) technique.

The classification of the frequency components of the events, having, without injection, a purely mechanical source can be done basically on the basis of the mechanical events related to the engine working conditions as, for example, those related to the engine distribution diagram: opening/closure of intake/exhaust valves of the cylinders other than the No. 4, opening/closure of injector needle, etc. This diagram is shown in Fig. 4. Beyond the recognizable events, angularly defined and directly related to engine working conditions, other events, whose origin is to be ascertained, are observed. Among them, it is possible to characterize the frequency components connected to the engine piston motion dynamic due to the piston impact on the cylinder liner,

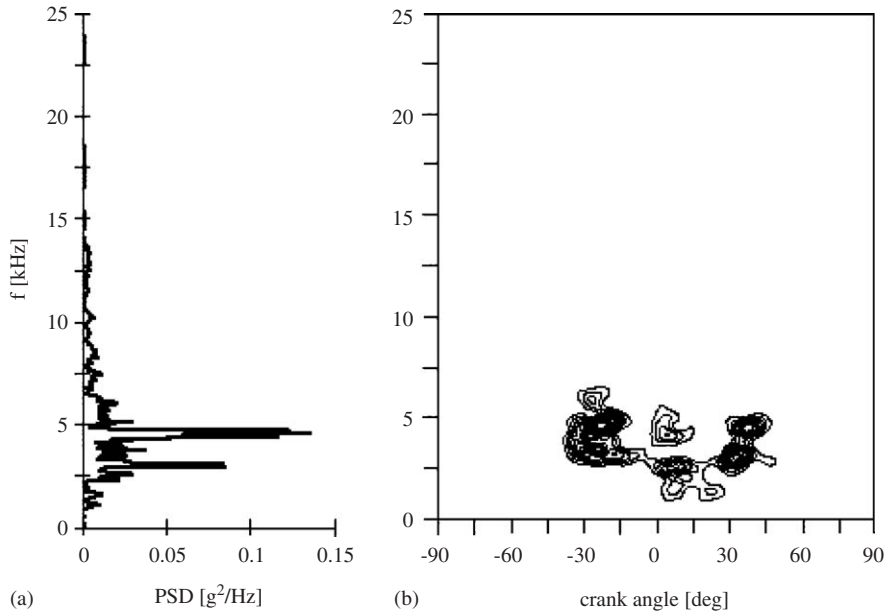

Fig. 5. Spectrogram (b) and PSD modulus (a) of vibration signal measured by accelerometer a_1 without fuel injection.

known as piston slap. In particular, it has been shown that this mechanical event takes place four times per revolution, at two angle intervals almost symmetric with respect to TDC and bottom dead center (BDC) [12]. Moreover, Haddad and Pullen [13] simulated the piston slap on a quiet engine using a force generator with hydraulic actuator. This generator reproduced exactly the force time shape and modulus induced by the lateral impact of the piston. Through this technique it was possible to detect the frequency interval of the engine vibration caused by the piston slap.

In Fig. 5 the spectrogram of the signal without injection is displayed; on the left, the PSD of the same signal is shown. It is important to underline that all plots showing spectrograms are adimensionalized with respect to the highest amplitude found on the same spectrogram. The analysis on the block vibration signal, without fuel injection (motored condition), is the baseline to be used with reference to the same signal measured in the presence of fuel injection and, therefore, combustion. In this way, it was possible to distinguish the mechanical components and to prove the physical origin of the frequency components related to the combustion process.

In Fig. 6 a spectrogram of the accelerometer a_2 signal is shown; on the left, the PSD of the same signal is displayed. From the analysis of the spectrograms in Figs. 5 and 6 it can be noticed, at angle intervals almost symmetric with respect to TDC, two frequency components centred at about 3.6 and 4.8 kHz on the vibration signals of both the accelerometers. The source of these components, on the basis of the angle interval at which they appear, can be ascribed to the piston slap. Similar results can be found in the work of Cho et al. [12]. In both the previous spectrograms, frequency components above 5 kHz are not present, in the angle interval in which, with fuel injection, the combustion takes place.

With fuel injected, the vibration signal characteristics vary. In fact, several high-frequency components (above 5 kHz), appear directly related to the corresponding in-cylinder frequency components. In Figs. 7 and 8, the comparisons between the PSD of pressure and accelerometer signals, without and with injection, are shown for three different speeds. The variation of the in-cylinder pressure signal frequency content, with fuel injection, is clear. It consists in the change of the intensity of the low-frequency components, strongly depending on the in-cylinder peak pressure, and of the middle–high components, which are related, on the contrary, to the rate of variation of the in-cylinder pressure curve and so to the sudden pressure increase due to the combustion of the premixed portion of the charge. The high-frequency components of the PSD of the in-cylinder pressure, in the presence of combustion, indicate the direct injection engine working conditions; in fact the typical dimensions of the combustion chamber of this kind of engines are smaller than those of indirect injection engines, this being the cause of the change of the natural resonant frequencies of the chamber.

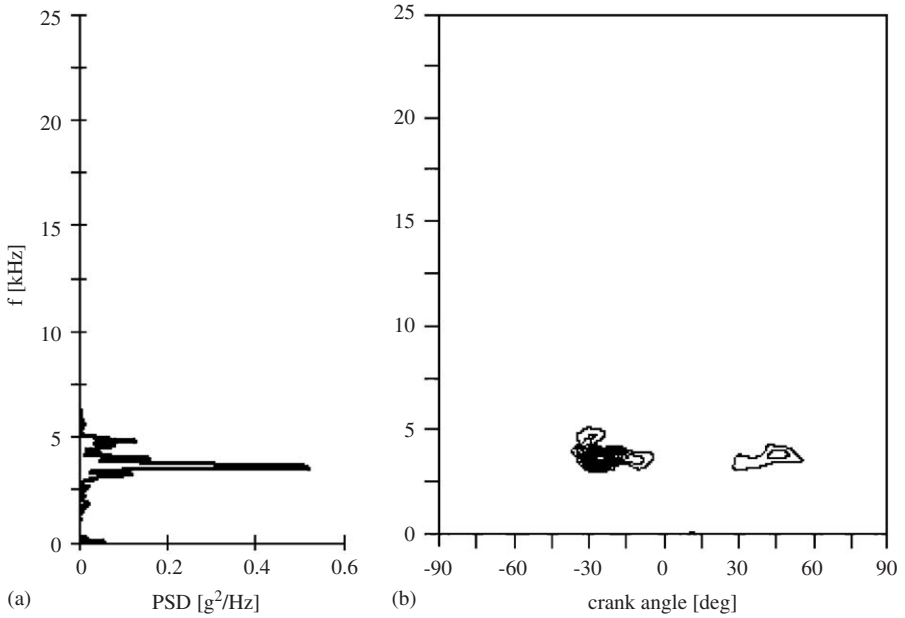

Fig. 6. Spectrogram (b) and PSD modulus (a) of vibration signal measured by accelerometer a_2 without fuel injection.

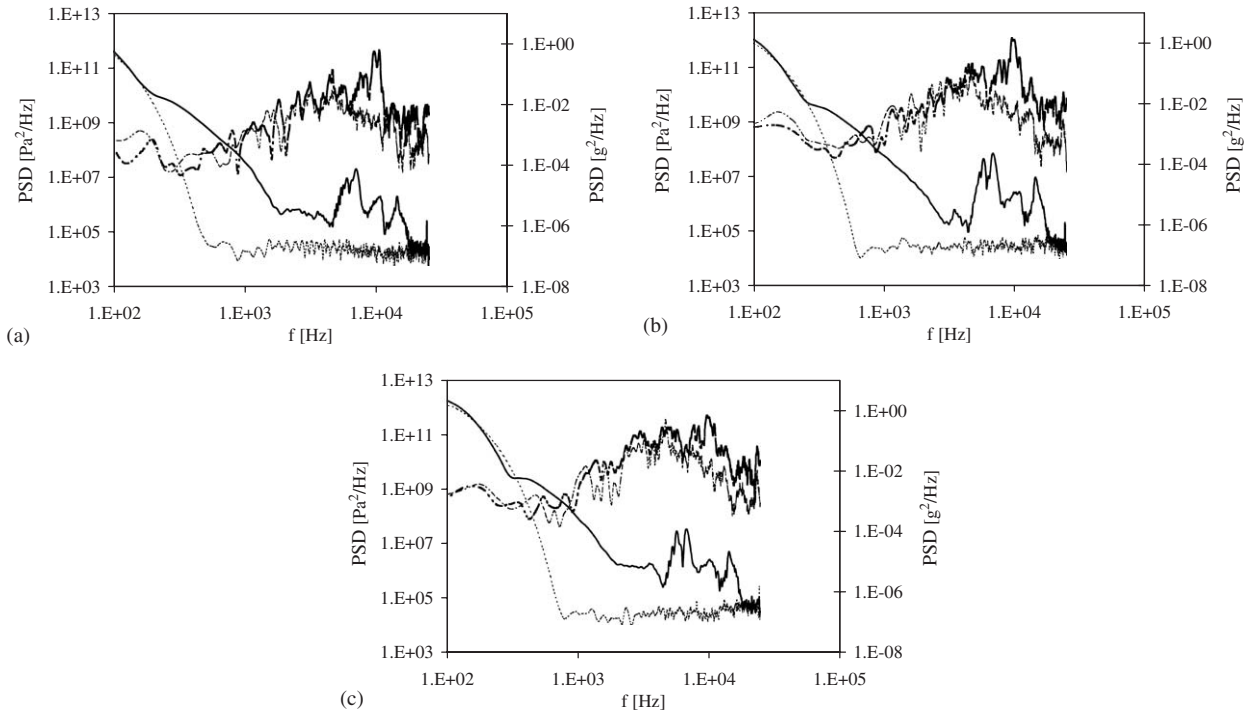

Fig. 7. PSD modulus of in-cylinder pressure without injection - - - - and with injection —— and of vibration signal measured by accelerometer a_1 without —··—·· and with injection ——·——· at 1200 rev/min (a), 1500 rev/min (b) and 1800 rev/min (c).

The angle location and the amplitude of the high-frequency peaks of the PSD, as Marples showed in Ref. [14], depend only on the amplitude fluctuations of the in-cylinder pressure due to the propagation of the steep fronted wave produced by the autoignition. The typical location of these fluctuation is around TDC.

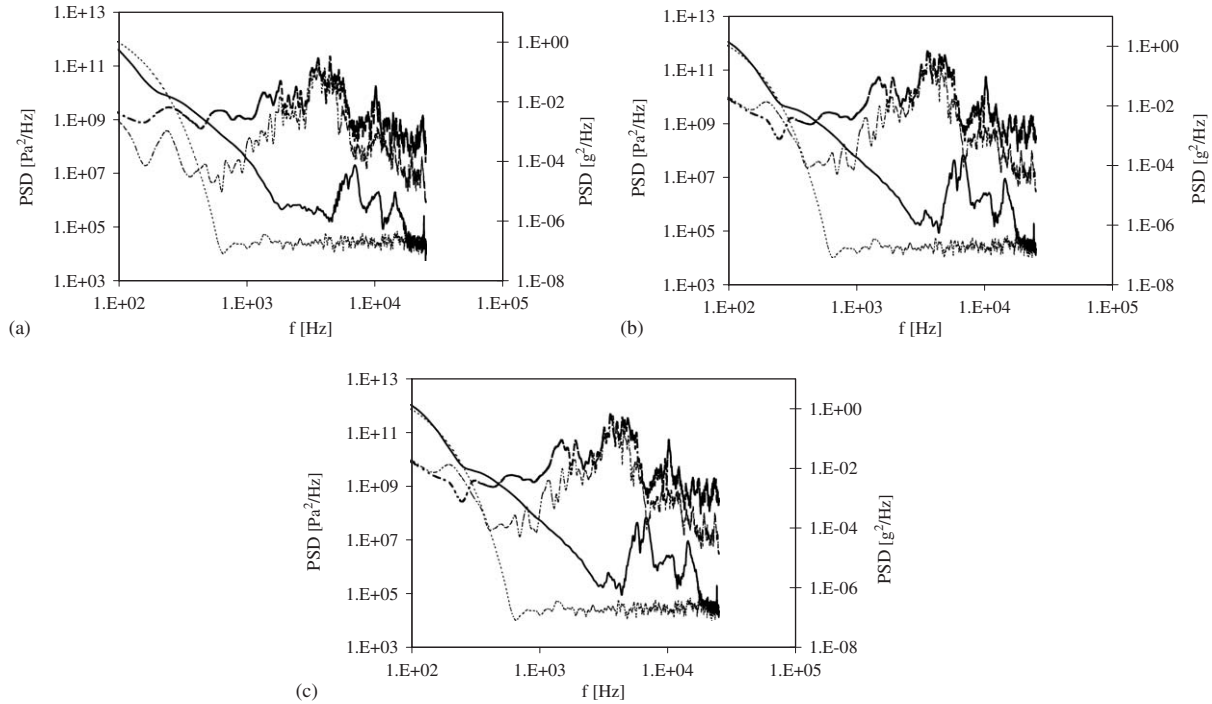

Fig. 8. PSD modulus of in-cylinder pressure without injection - - - - and with injection —— and of vibration signal measured by accelerometer a_2 without —··—·· and with injection ——·—— at 1200 rev/min (a), 1500 rev/min (b) and 1800 rev/min (c).

The PSD analysis of the vibration signal of the sensor placed on the side wall of the engine allows one to verify that the diagrams without and with injection (Figs. 5 and 6) are almost superimposable in the frequency interval below 5 kHz, verifying the mechanical origin of these components. Moreover, the two most relevant peaks, at about 3.6 and 4.8 kHz on the PSD of the signals without injection, placed almost in a symmetric way with respect to TDC and ascribed to piston slap, can be noticed. On the contrary, the PSD related to the signal from the accelerometer placed on the engine head, reveals that the detachment of the curves without and with injection is less evident, although it appears approximately in the same frequency interval.

A common aspect of the PSD of both accelerometer signals, very important for the subsequent part of the work and visible in Figs. 7 and 8, is the peak located at about 10 kHz (anyway included in the frequency interval 9–11 kHz), which is the most relevant in amplitude for the accelerometer a_1, while it is less evident for the accelerometer a_2. This peak is also present in the in-cylinder PSD although it is not the one with the greatest amplitude. The analysis of the position of the 10 kHz accelerometer signal peak, the absence of this frequency component in the same signal without injection together with the evidence of the corresponding peak of the in-cylinder pressure, leads to a certain identification of its source, which is the combustion process.

On the basis of the previous observations, it can be assumed that the accelerometer position on the side wall of the engine block is more suitable to obtain the frequency components related to the combustion process. In Fig. 9, the diagram of the difference between the PSD with and without injection, adimensionalized with respect to the case without injection, is shown, related to the accelerometer a_1 for three different engine speeds. The 9–11 kHz band significance in terms of sensibility to the combustion process is clear.

6. Pilot injection timing effect

The Pilot injection timing effect is shown in Fig. 10, related to the in-cylinder pressure and the block vibration signals from the two accelerometers. In the diagram in Fig. 10 the percentage variation of the

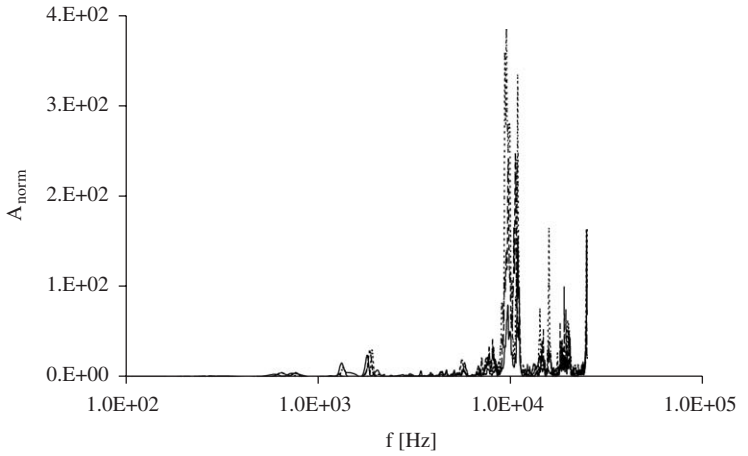

Fig. 9. Dimensionless diagram of the difference (A_{norm}) between the PSD modulus with and without injection for the vibration signal of the accelerometer a_1 at 1200 rev/min – – – –, 1500 rev/min - - - - and 1800 rev/min ——.

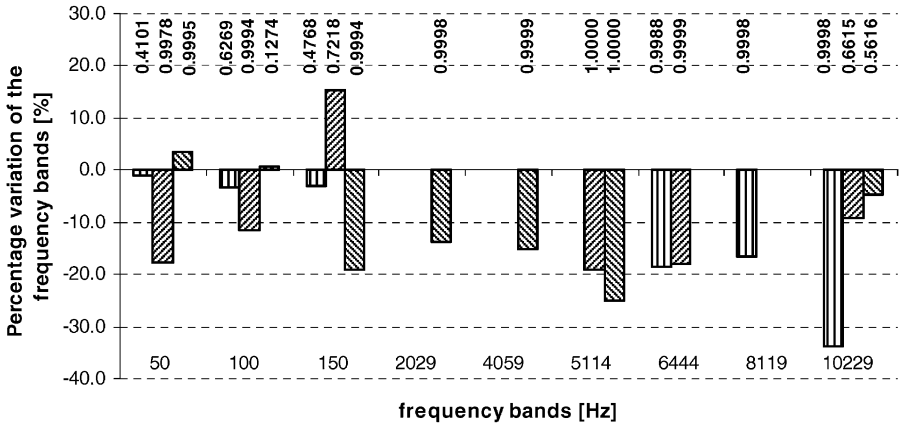

Fig. 10. Percentage variation of the amplitude of some meaningful frequency bands of the in-cylinder pressure and vibration signals from accelerometer a_1 and a_2, computed by the Fourier analysis varying AiP and significance levels of the factor computed by the ANOVA analysis. ▯, pressure; ▨, accelerometer a_1; ▧, accelerometer a_2.

amplitude of some significant frequency bands, varying the aforementioned parameter, of the in-cylinder pressure and vibration signals, obtained by the Fourier analysis, are shown.

The level of significance of the pilot injection timing variation on all the tested frequency bands has been estimated by means of the ANOVA analysis and the results are reported as labels above each of the analysed frequency bands in Fig. 10.

The choice of the frequency bands to be analysed, shown in Fig. 11, was carried out by means of a preliminary analysis of the signals spectra and it took into account both the frequency components directly related to the firing frequency, and those dependent on in-cylinder pressure fluctuations induced by the combustion process.

From the comparative analysis of the frequency bands of the pressure and the vibration signal from a_1 sensor, it can be observed that both the frequency bands 6444 and 10 229 Hz of the aforementioned signals are decreasing; however, the significance level of 10 229 Hz frequency band of the a_1 signal is low.

In a similar way, it can be noticed that the frequency components strongly related to mechanical events (2029–4059 Hz) in Fig. 10, related to a_2 sensor, show a clear decreasing trend. What is obtained from the

previous diagram analysis confirms that, in the limits of the assumed values of the pilot injection timing, the trend, in average, caused by an earlier pilot injection is a reduction of the vibration level. The reduction in amplitude of in-cylinder pressure high-frequency components, coherently observed on the corresponding accelerometer signal components, implies that a more advanced pilot injection, yet in the narrow limits assumed in the present work, leads to a change of the excitation conditions of the natural fluctuation modes of the charge inside the combustion chamber. In particular, it was observed that the pilot injection timing variation causes a variation of charge ignition nuclei position [15,16]; the more the delay in pilot injection

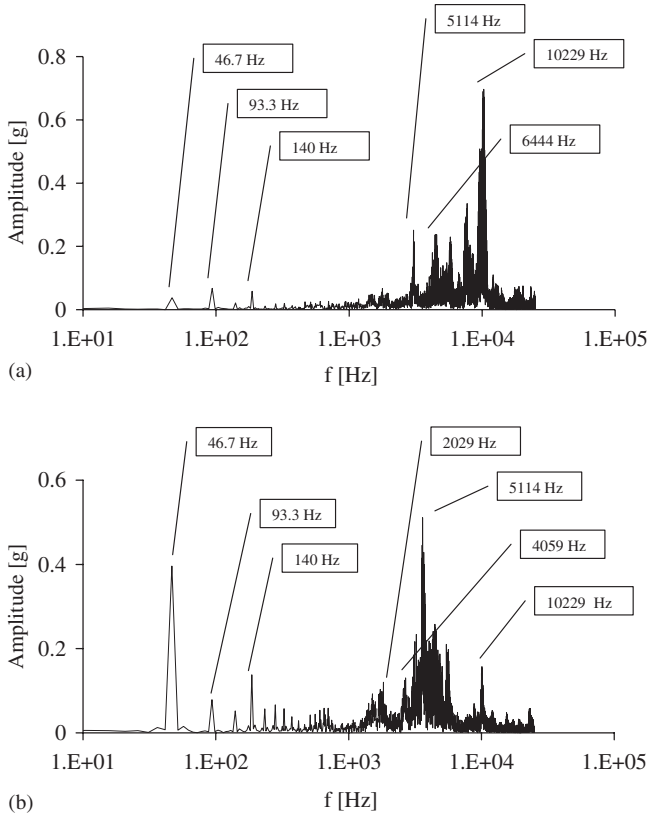

Fig. 11. Spectrum of accelerometer a_1 (a) and a_2 (b) signals, with highlighted meaningful frequency component.

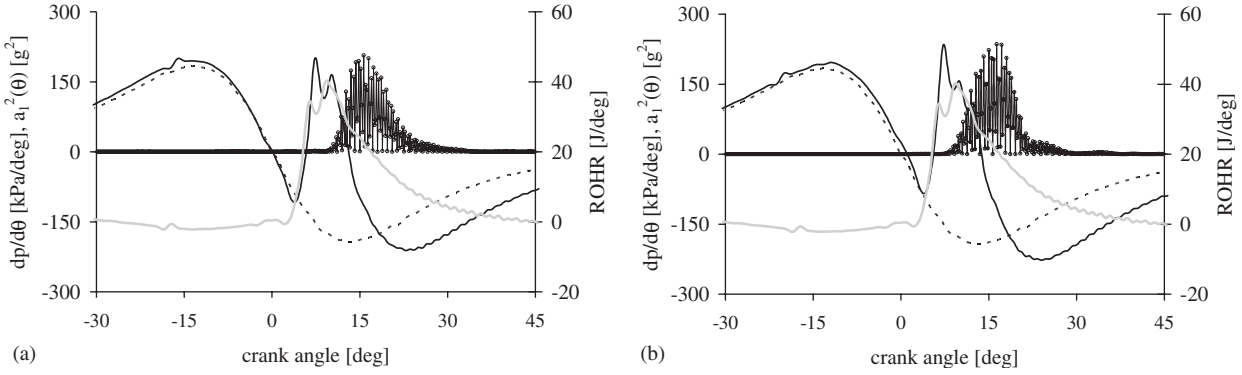

Fig. 12. In-cylinder pressure first derivative ($dp/d\theta$) without - - - and with fuel injection ——, accelerometer signal a_1 filtered in the frequency band 9–11 kHz and squared (a_1^2) —⊖— and ROHR ▬ for (a) 19/150/3/600 and (b) 23/150/3/600 tests.

timing, the nearer the first ignition nuclei to the injector nozzle. This is expected also because, delaying the pilot injection, a shorter pilot ignition delay is always observed [17]. Therefore, it can be assumed that, by varying pilot injection timing, the observed increase of the pressure amplitude can be related to a variation of the combustion propagation position.

The negligible variation of the in-cylinder pressure low-frequency components, not always in agreement with the trend showed by the corresponding low vibration signal components, coupled with the clear trend observed on the high components of all the analysed signals, give the characteristic "signature" caused by the AiP. This "signature" might be used to categorize the effects produced by this injection parameter from those related to other ones. This conclusion is important, in particular, if the narrow variation of AiP is taken in account.

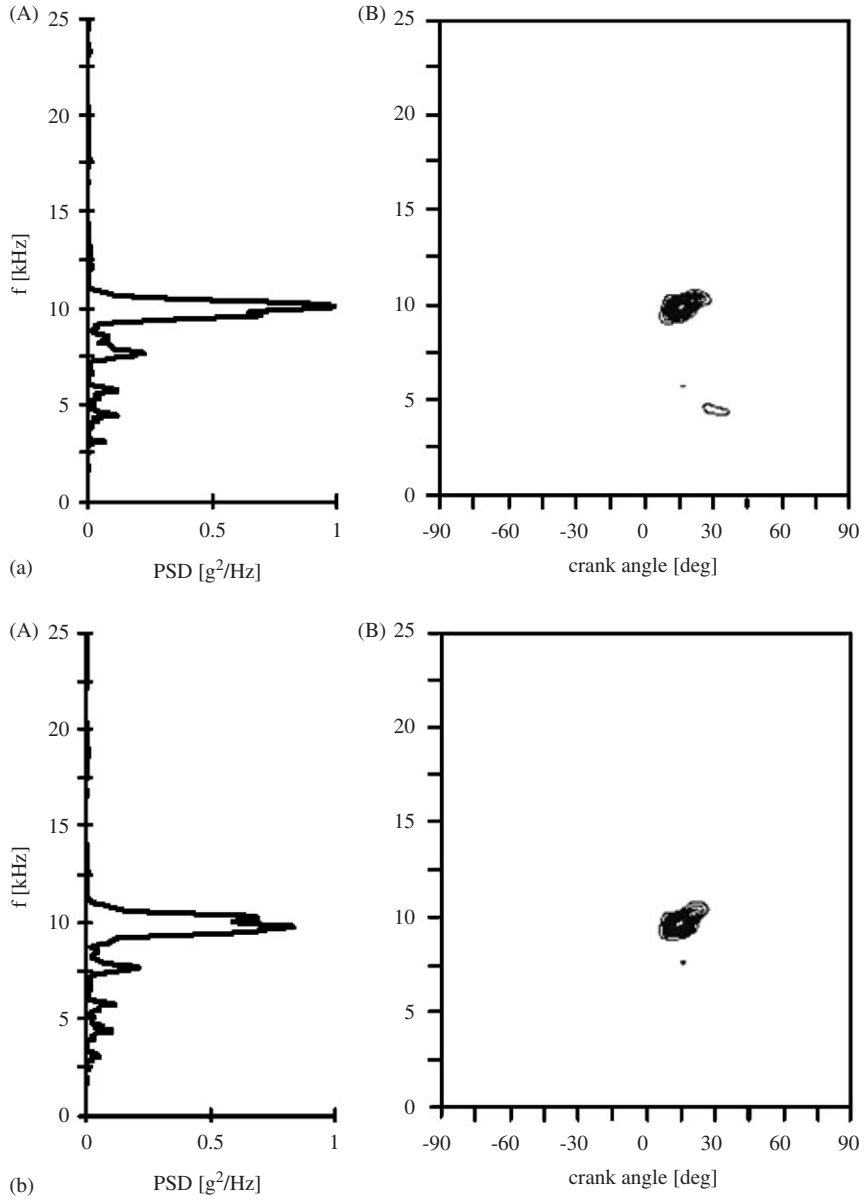

Fig. 13. Spectrogram (B) and PSD modulus of vibration signal measured by accelerometer a_1 (A) for (a) 19/150/3/600 and (b) 23/150/3/600 test.

What previously observed was obtained in terms of average trends, computed performing the average of the frequency band amplitude values of all the tests in which the analysed factor level was constant. Anyway, it is useful to thoroughly analyse what in average was observed, comparing the variation on the combustion process, monitored by the in-cylinder pressure first derivative and the ROHR, with the corresponding variations on the vibration signals.

The in-cylinder pressure first derivative and the ROHR, superimposed on that without injection, and the accelerometer signal a_1, filtered in the frequency band 9–11 kHz and squared, for two tests in which only AiP was varied, are shown in Fig. 12. The vibration signal spectrograms, related to the two aforementioned tests, are displayed on Fig. 13. In both diagrams of Fig. 12, the pilot injection does not burn before the main injection. This phenomenon is certainly to be ascribed to the very low quantity of pilot fuel injected (7.1% of the total fuel mass injected per cycle), resulting from the combination of the lowest injection duration (150 μs) and the lowest injection pressure value (60 MPa). The in-cylinder pressure first derivative curve detachment from the corresponding without injection, in both cases, is evident around 4 DCAATDC. In the same way, the accelerometer filtered squared signal increases, in both cases, starting at about 8.5 DCAATDC. The vibration signal delay is caused by the transmission time of the exciting pressure from the interior of the combustion chamber to the cylinder liner and finally to the outer surface of the engine block.

The increase of pilot injected fuel quantity, obtained raising the pilot injection duration (200 μs) (11% of the total fuel mass injected) and/or injection pressure (100 MPa) (22% and 15.4% of the total fuel mass injected), may lead to the autoignition of the pilot injection before the main injection start. This event is clearly shown by the 9–11 kHz band of the accelerometer a_1 reported in Fig. 14a, in which the accelerometer signal starts to increase just after the pilot injection combustion, visible by the analysis of the ROHR. The pilot ignition, instead, was not clearly detected when pilot injection was advanced (Fig. 14b). Fig. 15 shows the spectrogram of the same signal. By comparing parts (a) and (b) of the same figure, it can be observed that a delayed pilot injection, keeping constant the other factors, causes the PSD peak amplitude to increase. The trend of this peak, associated, as previously seen, to the combustion development, is in agreement with the trend shown by the peak, in the pressure first derivative, related to the pilot combustion.

These events, on the basis of the variation of the combustion conditions, can be attributed to the more favourable conditions, inside the combustion chamber, for the autoignition event. In fact, the temperature and in-cylinder pressure, at the start of pilot injection, are both higher when the pilot injection is delayed, because of the progress of the compression stroke. The increase of both temperature and pressure improves the conditions for fuel ignition, and so they affect the high increase of vibration level in the abovementioned frequency band. Therefore, through the vibration signal analysis, when varying pilot injection timing, a variation, matching that observed on pilot injection combustion, of both amplitude and timing of the accelerometer signal was obtained. These deductions were made for all tests at the highest level of injection

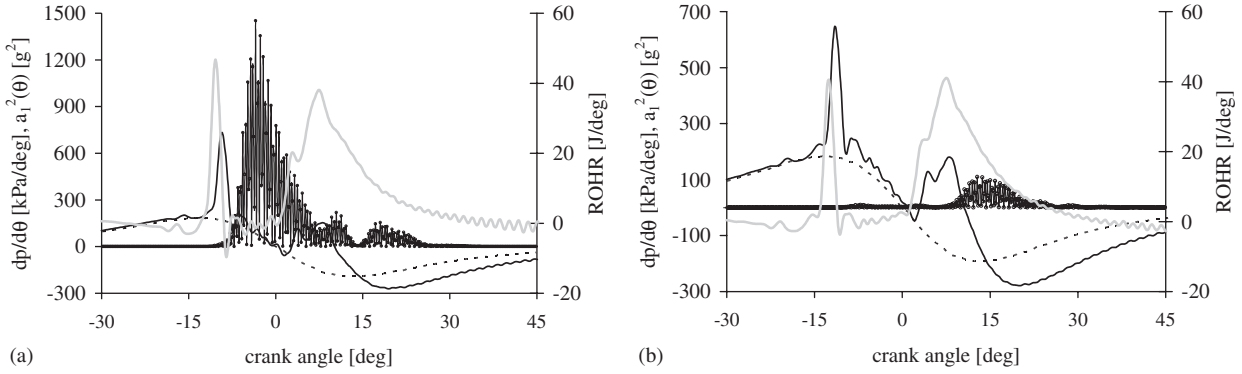

Fig. 14. In-cylinder pressure first derivative ($dp/d\theta$) without - - - and with fuel injection ——, accelerometer signal a_1 filtered in the frequency band 9–11 kHz and squared (a_1^2) —○— and ROHR ▬ for (a) 19/200/3/1000 and (b) 23/200/3/1000 test.

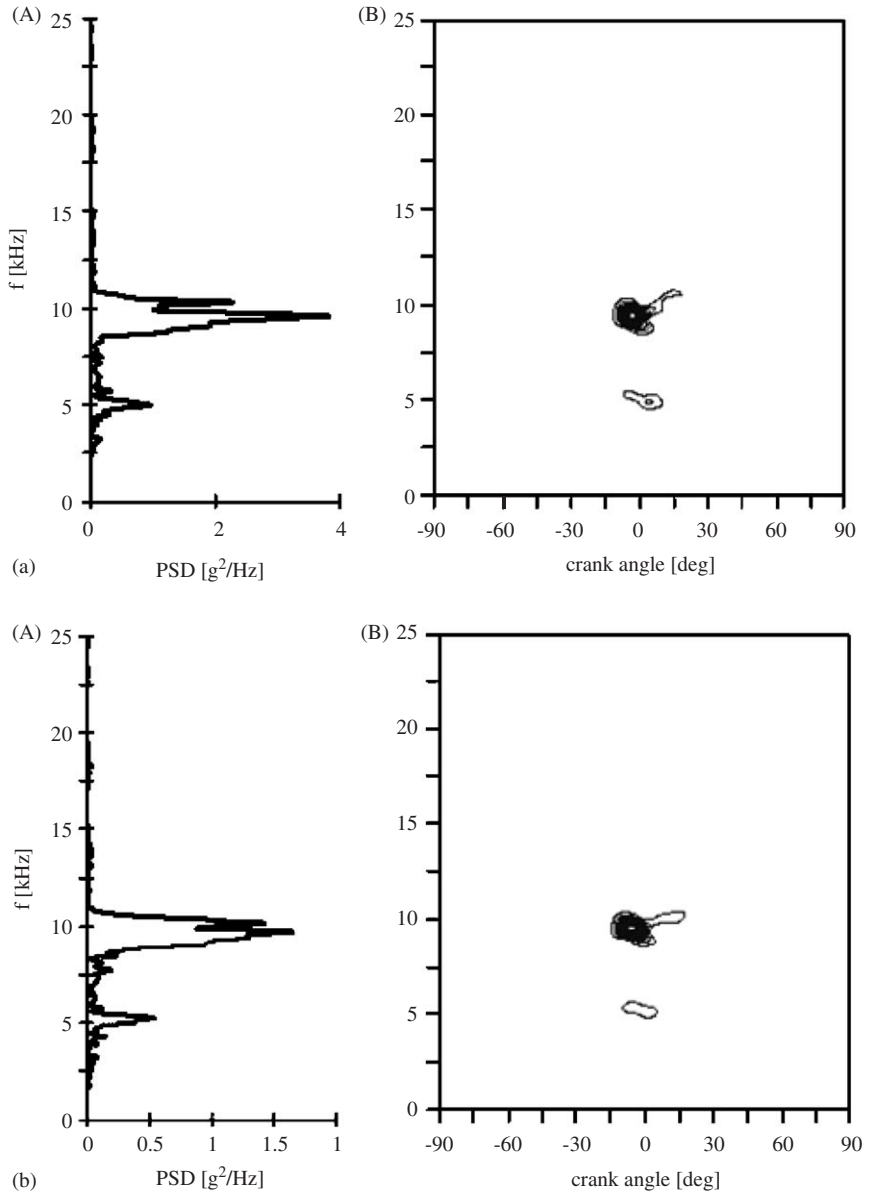

Fig. 15. Spectrogram (B) and PSD modulus of vibration signal measured by accelerometer a_1 (A) for (a) 19/200/3/1000 and (b) 23/200/3/1000 test.

pressure, leading to the conclusion that the increase of the value of this parameter contributes in raising the coherence between accelerometer signal and combustion process.

Given the well-established trend in the injection systems toward highest value of injection pressure, this trend is particularly encouraging on the effective applicability of this methodology.

7. Effect of the pilot injection duration

In general, the fuel-injected quantity results from the combination of injection pressure and the time interval of the needle opening, which is related to the energizing time of the solenoid of the electro-injector. The fuel quantities, as a function of ETP and p_{inj}, injected during the pilot injection are reported in Table 5.

Table 5
Pilot injection quantities

Tests	p_{inj} (MPa)	ETP (μs)	Pilot quantity (mm^3/cycle)	Percentage of pilot fuel mass to total (%)
1-3-9-11	60	150	1.3	7.1
2-4-10-12	100	150	2.8	15.4
5-7-13-15	60	200	2.0	11.0
6-8-14-16	100	200	4.0	22.0

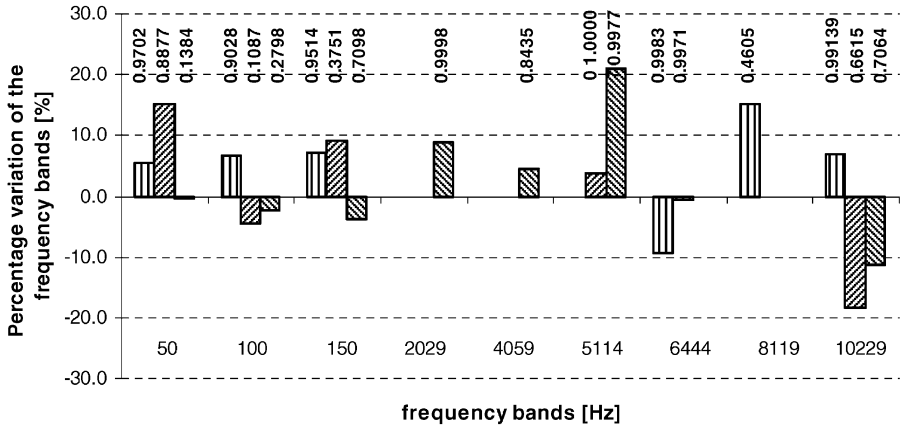

Fig. 16. Percentage variation of the amplitude of some meaningful frequency bands of the in-cylinder pressure and vibration signals from accelerometer a_1 and a_2, computed by the Fourier analysis varying ETP at the lowest level of p_{inj} and significance levels of the factor computed by the ANOVA analysis. ▯, pressure; ▨, accelerometer a_1; ▧, accelerometer a_2.

Pilot injection duration effect is shown in Figs. 16 and 17, which refer to the percentage variation of the aforementioned significant frequency bands of the in-cylinder pressure and cylinder block vibration, respectively, with $p_{inj} = 60$ and 100 MPa.

The level of significance of the pilot injection duration for each of the analysed frequency bands was estimated in average for all the p_{inj} levels, therefore the significance values, reported as labels in Figs. 16 and 17, do not vary.

It can be noticed that, for the lowest level of p_{inj} (Fig. 16), a negligible variation on the 10229 Hz of the in-cylinder pressure signal, and a decreasing trend on the 6444 Hz of the same signal were observed. A low dependency can be observed on the similar components of the a_1 signal at the lowest level of p_{inj} (Fig. 16), because of the small percentage variation of the frequency band amplitude. The same remarks can be made for a_2 signal at the lowest level of p_{inj} (Fig. 16). At the highest level of p_{inj}, varying ETP, a clear increasing trend of the 6444 and 10 229 Hz components can be observed, as in Fig. 17. This increasing trend can be coherently noticed on all the high components of signals a_1 and a_2 (Fig. 17). Based on what previously claimed, the ETP variation seems insignificant on the in-cylinder pressure components, at the lowest value of injection pressure. This result can be explained if the injected pilot quantities for the lowest level of p_{inj}, reported in Table 5, are analysed. For these tests, the pilot fuel quantity is too small to modify substantially the combustion process. In fact, as underlined in the work of Carlucci et al. [17], the concomitance of a small fuel quantity and a long ignition delay, implies a mixture too lean to burn, when thermodynamic conditions favourable for the autoignition are reached inside the combustion chamber.

The in-cylinder pressure first derivative, superimposed on the one related to the motored conditions, and the accelerometer a_1 squared signal, filtered in the frequency band 9–11 kHz are shown in Fig. 18, for two (19/150/0/600 and 19/200/0/600) of the tests with the lowest pilot injection quantities, given by the combination of the two values of ETP (150–200 μs) at the lowest value of p_{inj}. The spectrograms of the accelerometer signal, related to the aforementioned tests, are shown in Fig. 19.

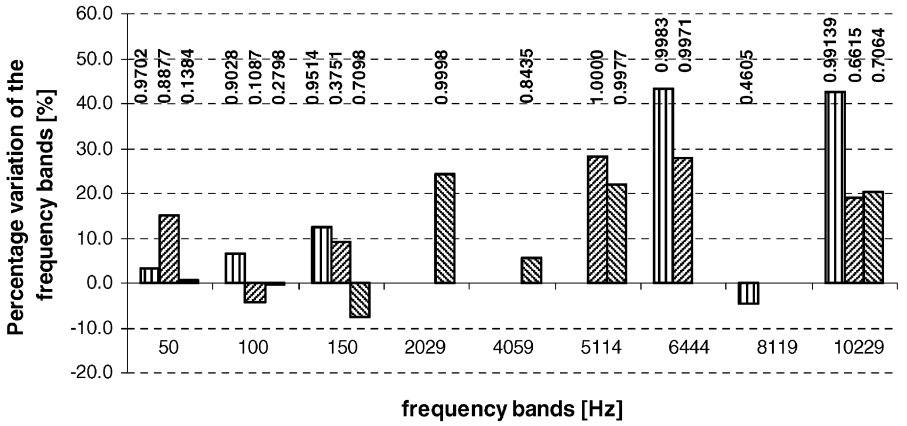

Fig. 17. Percentage variation of the amplitude of some meaningful frequency bands of the in-cylinder pressure and vibration signals from accelerometer a_1 and a_2, computed by the Fourier analysis varying ETP at the highest level of p_{inj} and significance levels of the factor computed by the ANOVA analysis. ▥, pressure; ▨, accelerometer a_1; ▧, accelerometer a_2.

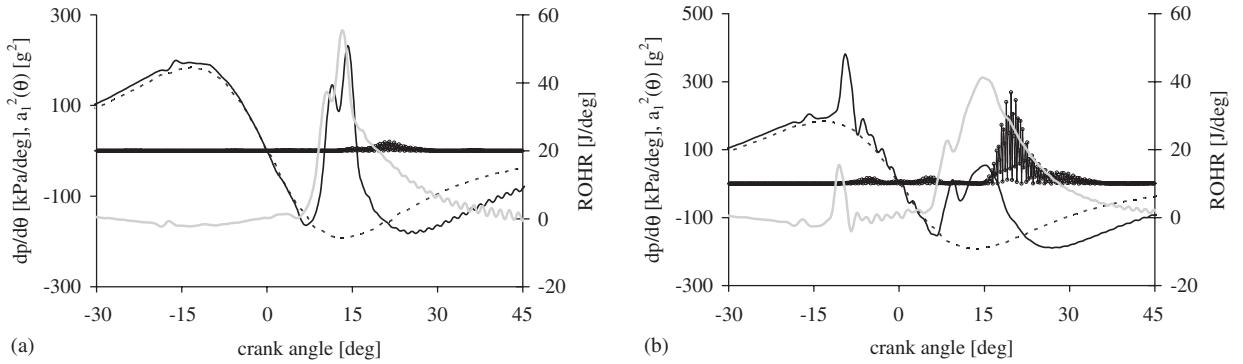

Fig. 18. In-cylinder pressure first derivative ($dp/d\theta$) without - - - and with fuel injection ——, accelerometer signal a_1 filtered in the frequency band 9–11 kHz and squared (a_1^2) —○— and ROHR ▬ for (a) 19/150/0/600 and (b) 19/200/0/600 test.

Although the pilot injection, for ETP of 200 μs, burns before the main injection, this fact can not be clearly observed on the accelerometer signal. Injecting with the lowest values of injection pressure and pilot duration, the pilot fuel does not burn. This results from the ROHR and is confirmed by the accelerometer signal, as it can be observed, for example, in Fig. 18a. On increasing the injection pressure to 100 MPa, and so raising pilot quantity, the accelerometer a_1 signal follows more consistently the in-cylinder pressure derivative, and ROHR, as reported in Fig. 20 and pointed out on angle scale in Fig. 21. In fact, the increase of the peak pressure derivative, related to pilot ignition and caused by the increase of energy release, also causes the increase of the accelerometer signal in the 9–11 kHz band.

Therefore, on the basis of the previous remarks, the accelerometer sensor can detect the pilot ignition and related combustion, when the pilot fuel releases a quantity of energy above a threshold. This conclusion is confirmed by Meissonier and Bazinet [18], who investigated the possibility of using the accelerometers in the field of common rail injection systems. In particular, the possibility to detect a small fuel quantity, whose combustion causes a vibration level detectable by the accelerometers, was investigated. This was carried out to test the different spraying behaviours of injectors with small structural differences due to the strict tolerance on their dimensions and so to act on the injection control system to smooth out the spraying differences and make their operation as uniform as possible.

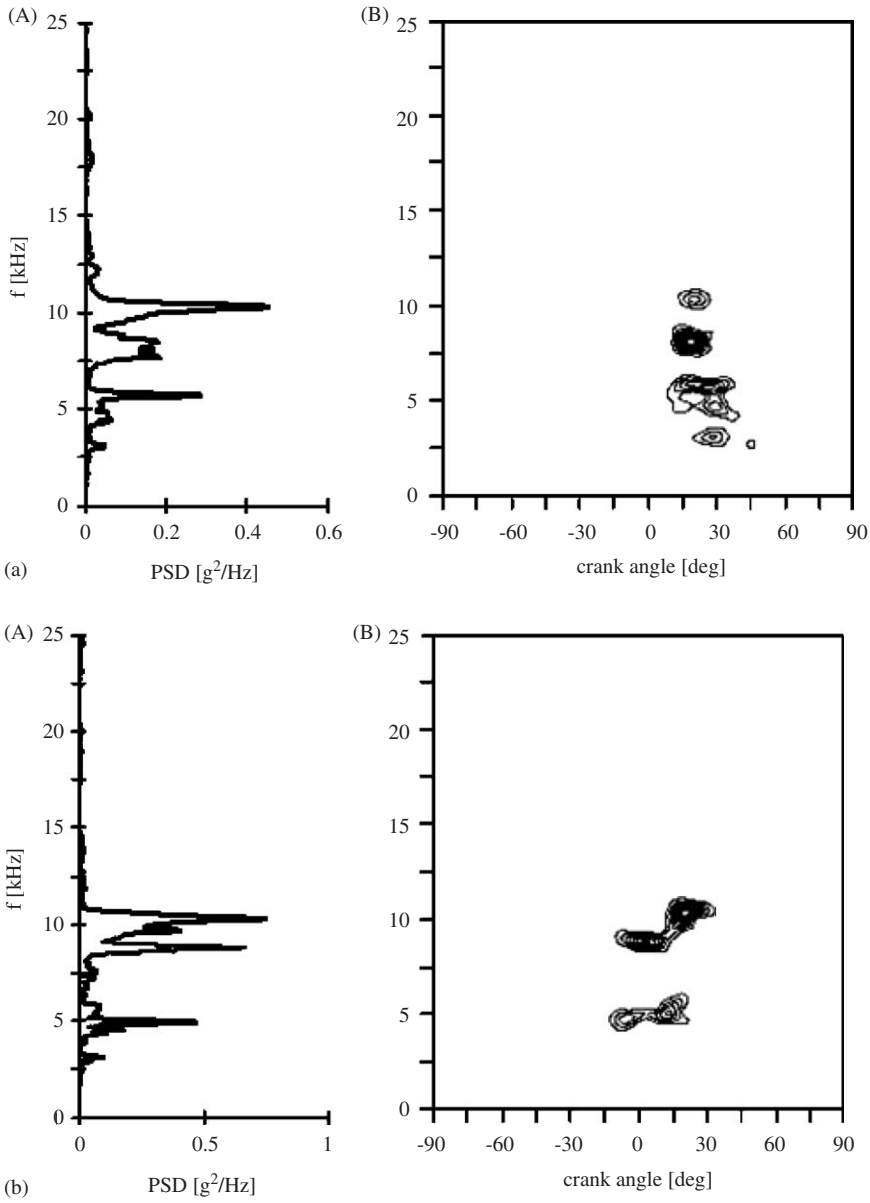

Fig. 19. Spectrogram (B) and PSD modulus of vibration signal measured by accelerometer a_1 (A) for (a) 19/150/0/600 and (b) 19/200/0/600 test.

Summarizing, pilot-injected quantity increase, causing, as main effect, the potential increase of the energy release, becomes really significant when fuel spray characteristics, like atomization, penetration and diffusion, strictly dependent on injection pressure value, assure the most favourable conditions for autoignition and combustion.

8. Injection pressure effect

The spray characteristics are strongly dependent on injection pressure. In particular, while increasing the injection pressure level, fuel droplets speed and, as a result, mass flow injected ($\dot{m}$) increase. In fact $\dot{m}$ varies

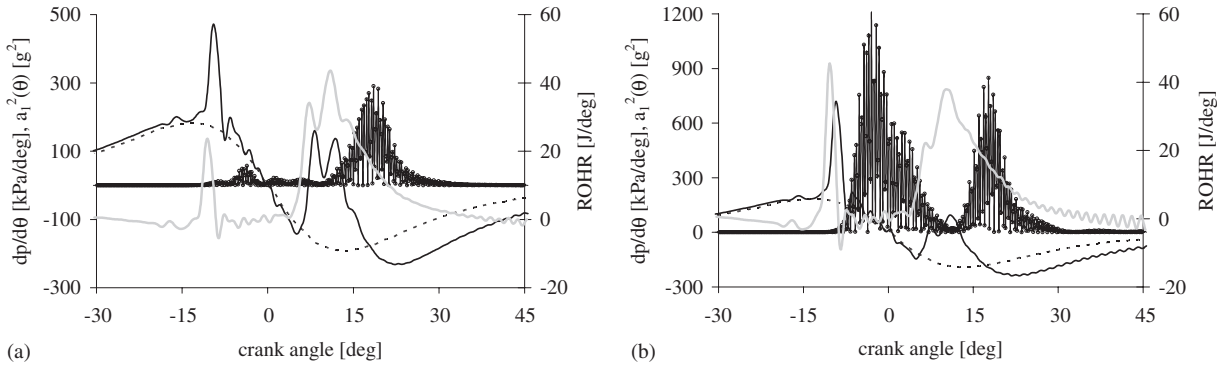

Fig. 20. In-cylinder pressure first derivative ($dp/d\theta$) without - - - and with fuel injection ——, accelerometer signal a_1 filtered in the frequency band 9–11 kHz and squared (a_1^2) —○— and ROHR ▬ for (a) 19/150/0/1000 and (b) 19/200/0/1000 test.

according to the following relation [10]:

$$\dot{m} = C_e \Omega \sqrt{\Delta p \rho_c}, \tag{7}$$

where Δp is the difference between fuel pressure at injector nozzle and in-cylinder pressure, C_e is efflux coefficient, Ω is the surface area of the injector holes and ρ_c is the volumetric mass of the fuel. Therefore, at highest injection pressure, the fuel spray penetrates more deeply in the combustion chamber before reaching the ignition conditions, causing wall impingement in smaller chambers. On the basis of the more reliable hypothesis, the fuel spray break-up is caused, by the aerodynamic interaction with the gas in the chamber, whose relative motion contributes to amplify unstable waves on the spray surface. Therefore, it can be assumed that the average droplets diameter depends, directly or indirectly, on several variables like the relative motion between the gas and the liquid (u_{rl}), the volumetric mass (ρ_l), viscosity (μ_l) and surface tension (σ_l), and the system geometry (diameter of injector holes, length of the injector nozzle). The average droplets diameter can be estimated by the following relation [10]:

$$d_g = C_d \left(\frac{2\pi\sigma_l}{\rho_g u_{rl}^2} \right) \lambda^*, \tag{8}$$

where C_d is a nearly unit constant, ρ_g is the gas volumic mass and λ^* is the dimensionless wavelength of the spray surface fluctuations.

An increase of the injection pressure reduces the fuel droplet's average diameter and then improves the spray formation promoting droplet vaporization. In particular, on raising the injection pressure, the relative speed of the spray increases according to the classical relation of a perfect liquid efflux:

$$u_{rl}^2 = 2\frac{\Delta p}{\rho_l}, \tag{9}$$

where Δp is the difference between fuel injection pressure and in-cylinder gas pressure.

On the basis of the previous remarks, the increase of the fuel injected during the ignition delay and the variation of physical characteristics of the spray, like reduction of droplets dimension and of their complete vaporization time, cause a premixed phase combustion more intense.

The effect of the variation of this factor is shown in Fig. 22, in which the significance levels from the ANOVA analysis are reported in labels as well. The injection pressure increase raises, in a significant way, all the analysed frequency components. In particular, the bands at the highest frequencies seem to be more affected by this parameter. This confirms that higher injection pressure, causing an increase of in-cylinder pressure derivative, are directly related to the modification of the thermodynamic conditions of the combustion process. The consistent increase of all the components of in-cylinder pressure can be attributed to

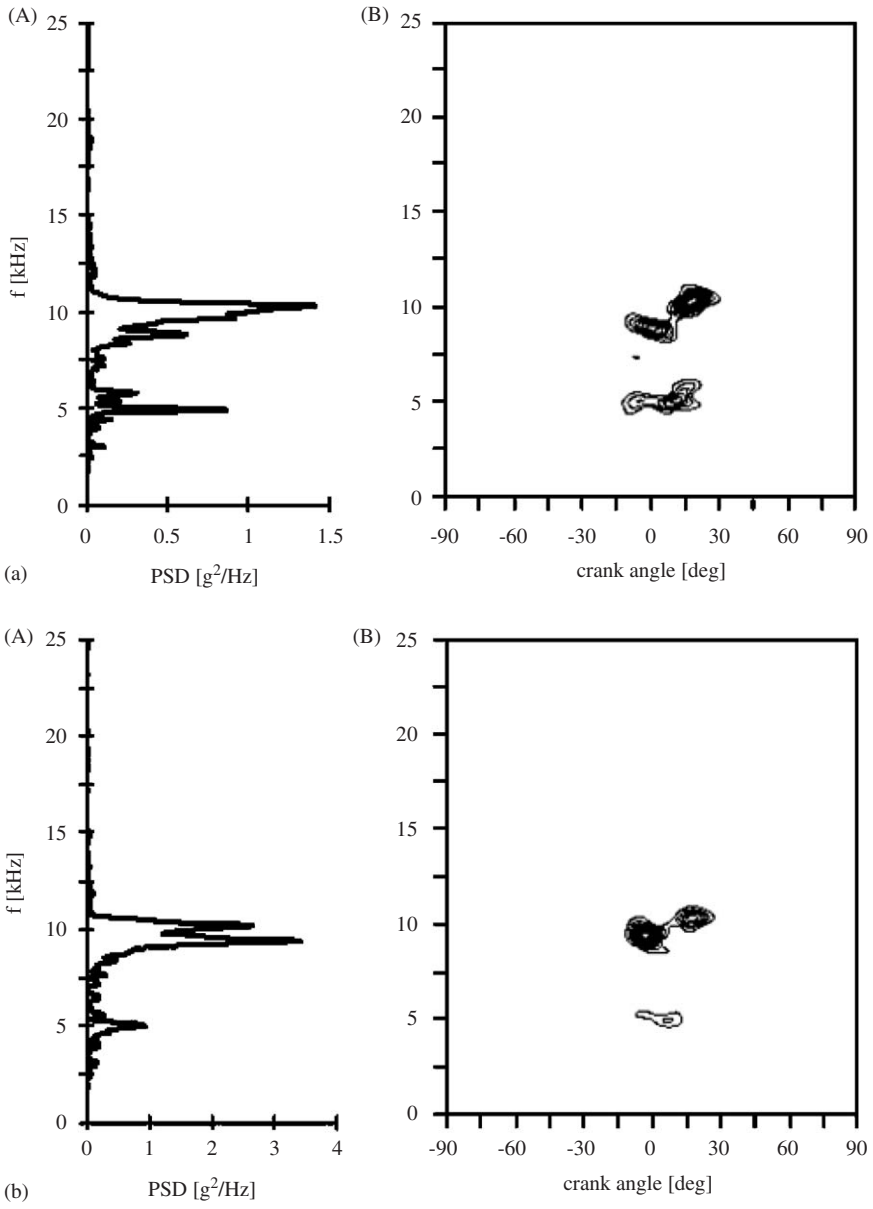

Fig. 21. Spectrogram (B) and PSD modulus of vibration signal measured by accelerometer a_1 (A) for (a) 19/150/0/1000 and (b) 19/200/0/1000 test.

a more impulsive initial combustion development. In fact, an ideal impulsive signal in time domain is reproduced in the frequency domain by a Fourier transform, in which all the frequency components are involved, and a real impulse gives more evidence to the highest components. Since the transfer function of the cylinder block is high for these components, they can be detected, in a clearer way, by the accelerometers.

The signature of the injection pressure variation is then unambiguous, being characterized by the increase of all the significant components of the analysed signals. This signature is also different from that imputable to pilot injection timing, which exclusively causes an increase of the highest components, and of the pilot injection quantity, at the highest level of injection pressure, which causes an increase of the low-frequency components.

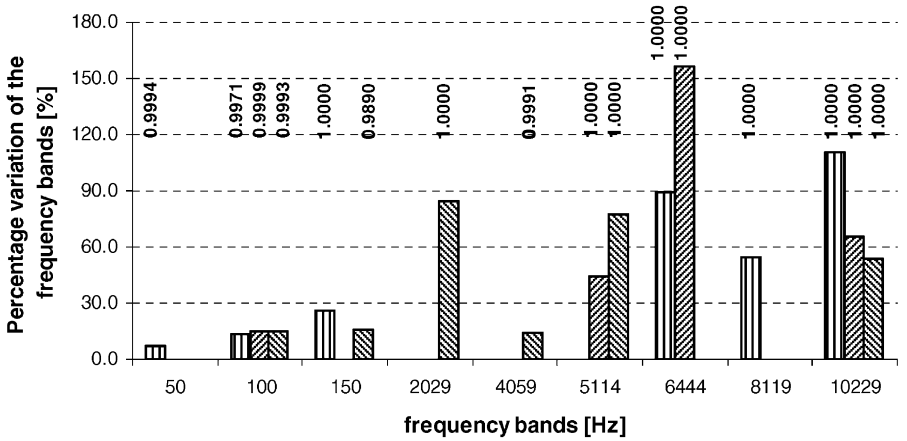

Fig. 22. Percentage variation of the amplitude of some meaningful frequency bands of the in-cylinder pressure and vibration signals from accelerometer a_1 and a_2, computed by the Fourier analysis varying ETP at the lowest level of p_{inj} and significance levels of the factor computed by the ANOVA analysis. ▥, pressure; ▨, accelerometer a_1; ▧, accelerometer a_2.

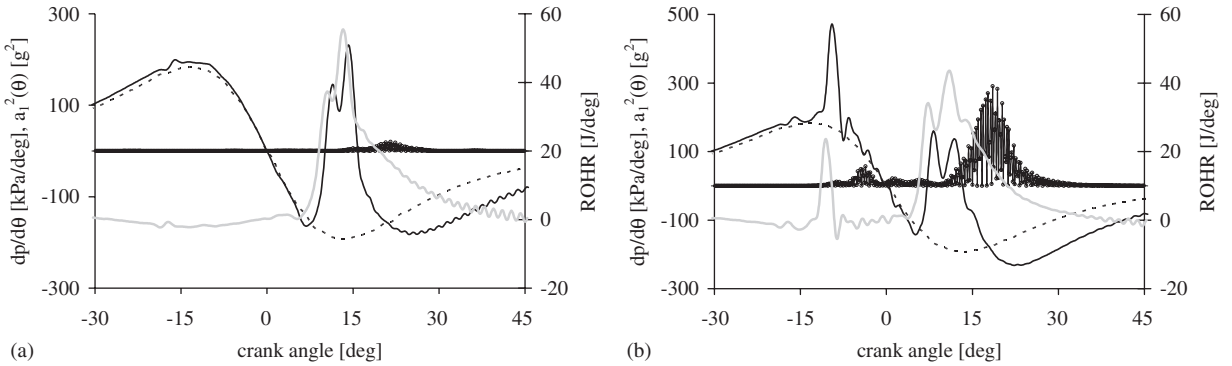

Fig. 23. In-cylinder pressure first derivative (dp/dθ) without - - - and with fuel injection ——, accelerometer signal a_1 filtered in the frequency band 9–11 kHz and squared (a_1^2) —○— and ROHR ▬ for (a) 19/150/0/600 and (b) 19/150/0/1000 test.

The injection pressure effect, as previously said, is clear for both the lowest (Figs. 23 and 24) and highest (Figs. 25 and 26) values of the pilot injection duration, causing a variation of at least one order of magnitude of the vibration signal amplitude.

The significance of this factor and the relative easiness through which it is possible to detect its effects from the outside, related to its double influence both on the physical formation conditions of the spray and on pilot injected fuel quantity, seems more useful for diagnostic aim than the other factors.

9. Conclusions

The influence of injection timing, pilot injection quantity and injection pressure on engine block vibration was evaluated. A complete three factor experimental plan varying the aforementioned injection parameters was realized.

In order to define in what way the combustion process development, varying the analysed injection parameters, modifies the engine block vibration signal, a preliminary analysis of the differences in the in-cylinder pressure and in the vibration signals with and without injection was realized by means of classical Fourier and time–frequency analysis. On the basis of the angle position, the frequency interval, in which the

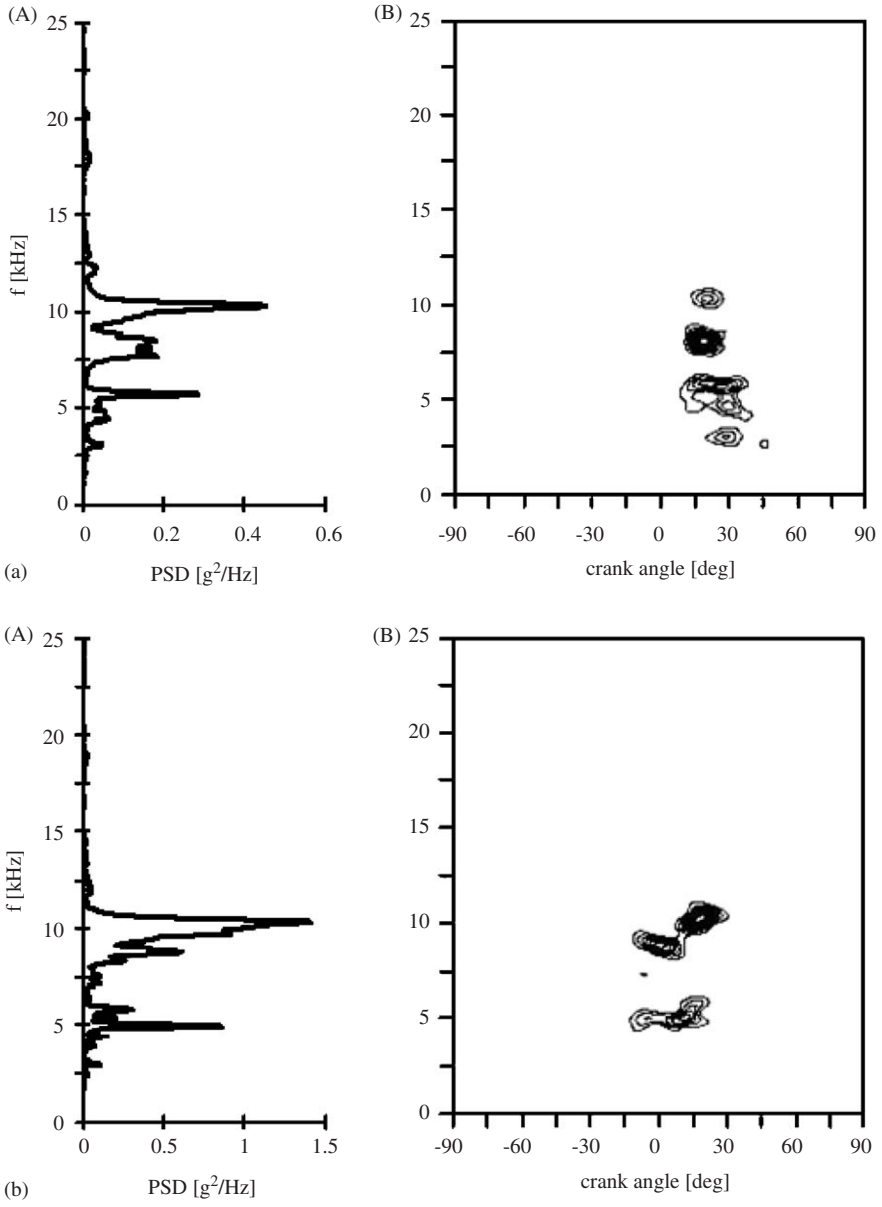

Fig. 24. Spectrogram (B) and PSD modulus of vibration signal measured by accelerometer a_1 (A) for (a) 19/150/0/600 and (b) 19/150/0/1000 test.

combustion process really affects the vibration signals, was determined. Moreover, through the time–frequency analysis, the piston slap was recognized among the mechanical phenomena.

An analysis based on some significant frequency bands of vibration and pressure signals was done to define a typical signature induced by the variation of each injection parameter. In particular, it was observed that the variations of pilot injection timing and duration at the highest level of the injection pressure, and of the same injection pressure, are detectable by the vibration signal. As a matter of fact, relating each trend of the frequency components with the angular characterization of the same components obtained by short-time Fourier transform analysis, it was possible to recognize a typical signature due to each parameter.

Moreover, to deeper investigate the relation between ''internal'' parameters, useful to describe the combustion process development, and the engine block vibration, the relation between a filtered accelerometer

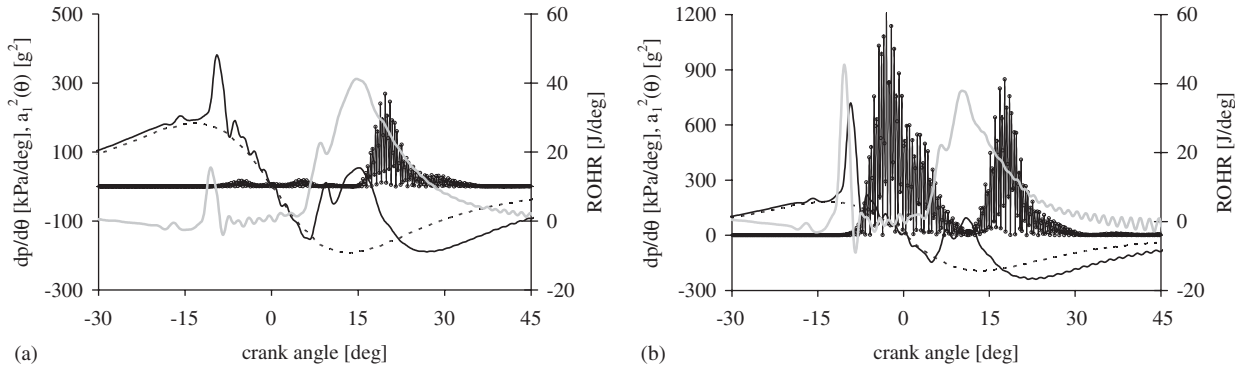

Fig. 25. In-cylinder pressure first derivative ($dp/d\theta$) without - - - and with fuel injection ——, accelerometer signal a_1 filtered in the frequency band 9–11 kHz and squared (a_1^2) —○— and ROHR ▬ for (a) 19/200/0/600 and (b) 19/200/0/1000 test.

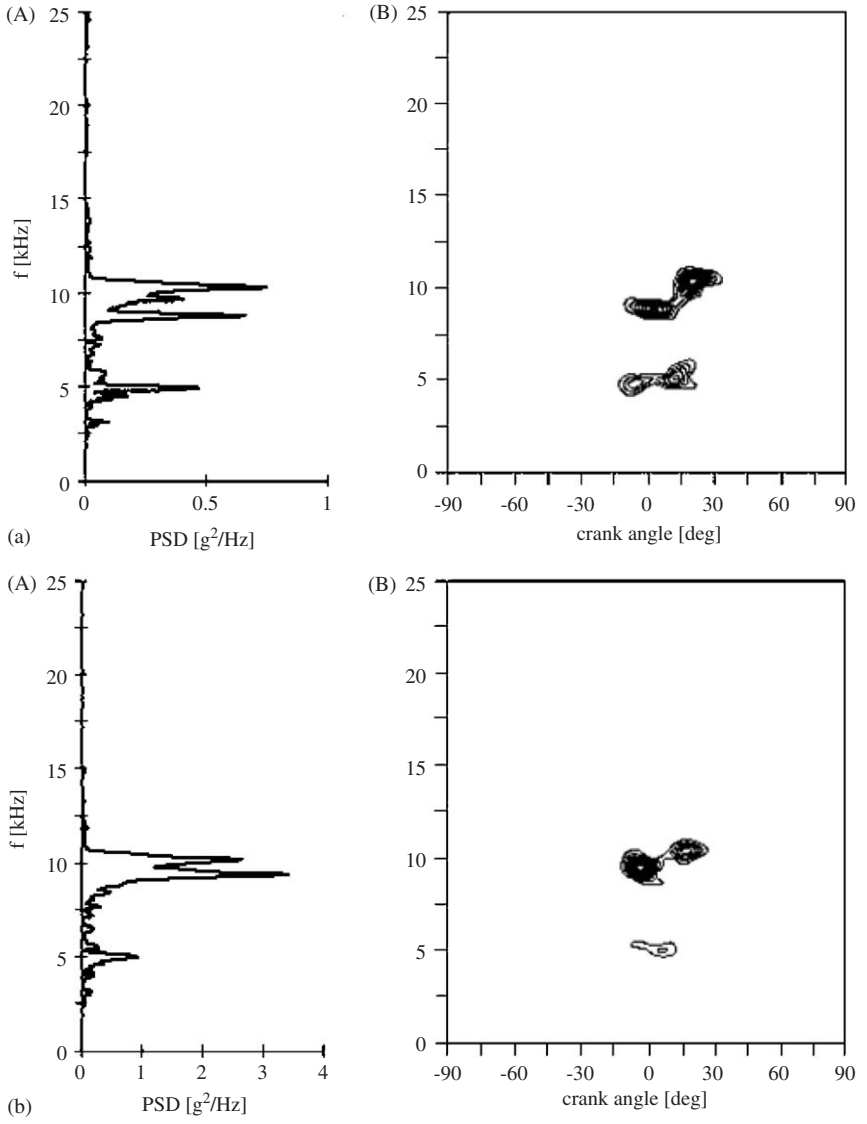

Fig. 26. Spectrogram (B) and PSD modulus of vibration signal measured by accelerometer a_1 (A) for (a) 19/200/0/600 and (b) 19/200/0/1000 test.

signal and the in-cylinder pressure first derivative and ROHR was studied. It was observed that at the highest level of injection pressure, both the pilot injection timing and duration variations can be outwardly detected, the first causing an amplitude increase and an angular advance, and the second the amplitude increase at the same angular position on the vibration signal, coherently to what was observed on in-cylinder pressure first derivative and rate of heat release. The injection pressure was always clearly detectable causing a coherent trend of the "internal" parameters and the vibration signals.

The paper has showed the possibility of relating the combustion development in diesel engine and the injection system correct functioning to the block vibration measurement. If, with further study and experimentation, a reliable relation between the variation of the engine parameters and the vibration signals is established, then these signals can be used to build cheap and useful diagnostic indicators. For example, a reliable control of the high-pressure injection pump operation, crucial component of the common rail injection system, achieved monitoring the combustion behaviour, could improve the engine operation reducing its maintenance costs. This goal is obtained using a relatively cheap diagnosis system, in particular if compared to the costs of a system based on the use of a pressure sensor inside the combustion chamber.

References

[1] P. Azzoni, G. Cantoni, G. Minelli, D. Moro, G. Rizzoni, M. Ceccarani, S. Mazzetti, Measurement of engine misfire in the Lamborghini 533 V-12 engine using crankshaft speed fluctuations, *Society of Automotive Engineers* Paper No. 950837, 1995.
[2] F. Gu, W. Li, A. D. Ball, A. Y. T. Leung, The condition monitoring of diesel engines using acoustic measurements—part 1: acoustic characteristics of the engine and representation of the acoustic signals, *Society of Automotive Engineers* Paper No. 2000-01-0730, 2000.
[3] A. D. Ball, F. Gu, W. Li, The condition monitoring of diesel engines using acoustic measurements—part 2: fault detection and diagnosis, *Society of Automotive Engineers* Paper No. 2000-01-0368, 2000.
[4] K. M. Chun, K. W. Kim, Measurement and analysis of knock in a SI engine using the cylinder pressure and block vibration signals, *Society of Automotive Engineers* Paper No. 940146, 1994.
[5] G. Zurita, V. A. Ågren, E. Pattersson, Reconstruction of the cylinder pressure from vibration measurements for prediction of exhaust and noise emissions in ethanol engines, *Society of Automotive Engineers* Paper No. 1999-01-1658, 1999.
[6] M.O. Othman, Improving the performance of a multi-cylinder engine by spectrum analyzer feedback, *Journal of Sound and Vibration* 131 (1) (1989) 1–11.
[7] J. Antoni, J. Daniere, F. Guillet, Effective vibration analysis of IC engines using cyclostationarity—part I: a methodology for condition monitoring, *Journal of Sound and Vibration* 257 (5) (2002) 815–837.
[8] K. Schmillen, J. Wolschendorff, Cycle to cycle variations of combustion noise in diesel engines, *Society of Automotive Engineers* Paper No. 890129, 1989.
[9] C. A. Blunsdon, J. C. Dent, Modelling the source of combustion noise in a direct-injection diesel engine using CFD, *Society of Automotive Engineers* Paper No. 941898, 1994.
[10] J.B. Heywood, *Internal Combustion Engine Fundamentals*, McGraw-Hill, New York, 1988.
[11] J.S. Bendat, A.G. Piersol, *Engineering Applications of Correlation and Spectral Analysis*, Wiley, New York, 1993.
[12] S.-H. Cho, S.-T. Ahn, Y.-H. Kim, A simple model to estimate the impact force induced by piston slap, *Journal of Sound and Vibration* 255 (2) (2002) 229–242.
[13] S.D. Haddad, H.L. Pullen, Piston slap as a source of noise and vibration in diesel engines, *Journal of Sound and Vibration* 34 (2) (1974) 249–260.
[14] V. Marples, On the frequency content of the surface vibration of a diesel engine, *Journal of Sound and Vibration* 52 (3) (1977) 365–386.
[15] L. Ricart, R. D. Reitz, Visualization and modeling of pilot injection and combustion in diesel engines, *Society of Automotive Engineers* Paper No. 960833, 1996.
[16] T. Tanaka, A. Ando, K. Ishizaka, Study on the pilot injection of diesel engine using common-rail injection system, *Japanese Society of Automotive Engineers* (*Review*) 23 (2002) 297–302.
[17] P. Carlucci, A. Ficarella, D. Laforgia, Effects of pilot injection parameters on combustion for common rail diesel engines, *Society of Automotive Engineers 2003 Transactions*, *Journal of Engines* Paper No. 2003-01-0700, 2003.
[18] G. Meissonnier, V. Bazinet, Injection control in an advanced common rail fuel injection system, *ATA* 54 (1/2) (2001) 12–20.